Available online at www.sciencedirect.com

ScienceDirect

IFAC PapersOnline CONFERENCE PAPER ARCHIVE

IFAC PapersOnLine 54-11 (2021) 79–84

Reconstructing faulty measurements at a tailings treatment surge tank

K. Sekila [*], **J. D. le Roux** [*,1]

[*] *Department of Electrical, Electronic and Computer Engineering, University of Pretoria, Pretoria, South Africa*

Abstract: Measurement faults in processing plants can cause the performance of a process to deteriorate. Once the failure of a sensor is identified, it is possible to reconstruct the missing measurement using the measurements of other sensors. Plant operators or controllers can use the reconstructed measurement to make informed decisions. Although the theory to reconstruct faulty measurements is well-developed, various issues remain when applying the method in practice. In this study, a tailings treatment surge tank, which is a very simple process, is used to investigate issues surrounding measurement reconstruction using Principal Component Analysis. Different sets of faulty and correct sensors were created to investigate measurement reconstruction accuracy. The state observability of the surge tank model states was compared to the ability to reconstruct faulty measurements. It was found that the system does not necessarily need to be observable in terms of the available correct measurements for successful reconstruction. In addition, a fault in the measurement of the volume of slurry in the tank could not be reconstructed, even if it was the only faulty measurement. This indicates that the success of measurement reconstruction by Principal Component Analysis may depend on the dynamics of the process and the associated model.

Keywords: Fault Detection and Isolation, Measurement Reconstruction, Observability, Principal Component Analysis, Process Control, Sensor Validation.

1. INTRODUCTION

To achieve the optimal economic benefits through advanced process control in mineral processing plants, accurate and reliable measurements are necessary. Although there is an array of sensors taking measurements, the sensors are subject to various faults. Since these measurements are used in subsequent advanced process control strategies, any faulty measurements will reduce the performance of the plant. Fault Detection and Isolation (FDI) and reconstruction are mandatory prerequisites before the measurements are used for advanced process control. The progression from fault detection to fault isolation to fault reconstruction can be regarded as sensor validation (Hodouin, 2011; Brooks and Bauer, 2018).

Common measurement faults in mineral processing industries include: bias, precision degradation, drift or complete failure of the sensor. There are various methods to detect these faults which include univariate control charts, model residuals, or multivariate statistical analysis. Multivariate statistical analyses include Principal Component Analysis (PCA), parity equations, minimal mean square error estimation, and independent component analysis. Fault isolation can be achieved through contribution analysis, missing variable approach, or probability quantification. Once a fault is detected and isolated, the sensor fault can be reconstructed or corrected through optimisation-based, regression-based, or machine learning methods (Kerschen et al., 2005; Kullaa, 2010; Qin, 2012; Yi et al., 2017).

Although the methodology to reconstruct faulty measurements has been available for many decades, Brooks and Bauer (2018) report that few commercial solutions are available. Of those available, Brooks and Bauer (2018) used a package which uses a PCA approach based on the work of Qin and Weihua (1999) (cf. Qin and Guiver (2003)). The package solution is applied to operating data from a mineral processing plant with persistent sensor problems. Very poor measurement reconstruction was achieved even after numerous attempts to improve reconstructability. Brooks and Bauer (2018) conclude that it is not necessarily the algorithm, but rather the choices surrounding data selection and appropriate filtering which influence the measurement reconstruction performance.

The aim of this study is to investigate the relation between the available correct measurements at a plant and the reconstruction of faulty measurements. A static PCA reconstruction method is applied to reconstruct multiple faults (Qin and Weihua, 1999; Dunia and Qin, 1998; Qin and Guiver, 2003). The method is applied to a tailings treatment surge tank. A simulation model of the surge tank is used to generate data. The state-observability of the surge tank model is analysed to evaluate if observability provides insight into which measurements can be reconstructed. For the purposes of this study, it is assumed that faults were already detected and the faulty sensors were already identified.

This paper is organised as follows: Section 2 details the surge tank model, Section 3 describes the observability analysis of the surge tank model, Section 4 explains recon-

[1] Corresponding author. E-mail: derik.leroux@up.ac.za

10.1016/j.ifacol.2021.10.054

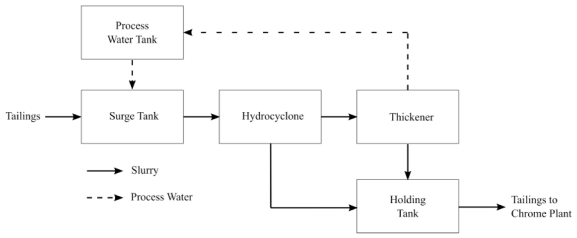

Fig. 1. Flowsheet of the BTT plant.

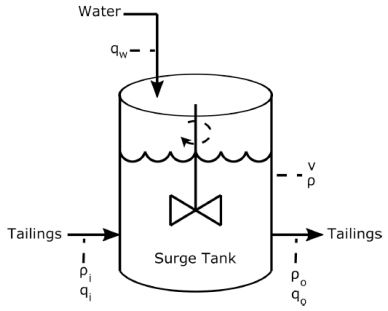

Fig. 2. Surge tank schematic.

struction by means of PCA, Section 5 outlines the measurement reconstruction experiments, Section 6 provides a brief discussion of results, and Section 7 concludes the paper.

2. TAILINGS TREATMENT SURGE TANK MODEL

2.1 Process description

The process simulated in this paper is a surge tank which forms part of an industrial bulk tailings treatment (BTT) plant. The flowsheet of the BTT plant is depicted in Fig. 1. The central aim of the BTT plant is to provide the downstream chrome concentrator with a stable feed density. The surge tank uses process water to maintain a stable feed density. If the feed does not have a stable density, it compromises the efficiency of the downstream hydrocyclone and thickener (Burchell and Craig, 2019).

2.2 Surge tank process model

A brief description of the model of the BTT surge tank as shown in Fig. 2 is shown here. The model variables and their nominal operating condition values for the surge tank model is given in Table 1.

Table 1. Model variables and nominal operating values.

Variables	Nominal	Description
Manipulated Variables		
q_i $[m^3/h]$	600	Flowrate of slurry from the tailings
q_w $[m^3/h]$	150	Flowrate of water into the tank
q_o $[m^3/h]$	750	Flowrate of slurry out of the tank
Controlled Variables		
v $[m^3]$	10	Volume of the tank
ρ $[t/m^3]$	1.4	Density of slurry in the tank
Disturbances		
ρ_i $[t/m^3]$	1.5	Density of slurry from tailings

Assuming perfect mixing within the surge tank, the dynamic process model can be derived from a mass balance of the surge tank:

$$\frac{d\rho v}{dt} = \rho_i q_i + q_w - \rho q_o, \tag{1}$$

where ρ_i is the density of slurry from the tailings, q_i is the flow rate of slurry from the tailings entering the tank, q_w is the flow rate of water entering the tank, ρ is the density of slurry in the tank, q_0 is the flow rate of slurry out of the tank, and v is the volume of slurry in the tank. (It is assumed the density of slurry exiting the tank ρ_o is equal to ρ.)

Assuming the volume stays constant during mixing, the volume balance of the surge tank is described as:

$$\frac{dv}{dt} = q_i + q_w - q_o. \tag{2}$$

Eq. (1) can be expanded as:

$$v\frac{d\rho}{dt} + \rho\frac{dv}{dt} = \rho_i q_i + q_w - \rho q_o. \tag{3}$$

Combining (2)-(3) produces a nonlinear state space model:

$$\begin{bmatrix} \dot{v} \\ \dot{\rho} \end{bmatrix} = \begin{bmatrix} q_i + q_w - q_o \\ \dfrac{q_i\rho_i - \rho(q_i + q_w) + q_w}{v} \end{bmatrix}. \tag{4}$$

The model in (4) is linearised around the nominal operating condition shown in Table 1 and represented as a transfer function:

$$\begin{aligned} Y(s) &= G_p(s)U(s) + G_d(s)D(s) \\ &= \begin{bmatrix} \dfrac{1/s}{0.01} & \dfrac{1/s}{s+75} \\ \dfrac{-0.04}{s+75} & \end{bmatrix} U(s) + \begin{bmatrix} 0 \\ \dfrac{60}{s+75} \end{bmatrix} D(s), \end{aligned} \tag{5}$$

where $Y(s) = \mathcal{L}\{[v\ \rho]^T\}$, $U(s) = \mathcal{L}\{[q_w\ q_i]^T\}$, $D(s) = \mathcal{L}\{\rho_i\}$ and $\mathcal{L}\{\cdot\}$ is the Laplace operator.

3. OBSERVABILITY

3.1 Observability for a nonlinear system

A multi-input-multi-output control-affine nonlinear state-space model with $\dim(x) = n$ and $\dim(y) = m$ can be written as:

$$\begin{aligned} \dot{x} &= f(t,x) + g(t,x)\,u \\ y &= h(t,x) \end{aligned} \tag{6}$$

The system in (6) is said to be locally (weakly) observable at x_0 if there exists a neighbourhood X_0 of x_0 such that for every x_1 which is an element of the neighbourhood $X_1 \subset X_0$ of x_0 the indistinguishability of the states x_0 and x_1 implies that $x_0 = x_1$. The two states x_1 and x_0 are said to be indistinguishable if for every admissible input u the output function y of (6) for the initial state x_0 and for the initial state x_1 is identical. If the system satisfies the so called observability rank condition, i.e. the observability codistribution (Hermann and Krener, 1977):

$$\mathcal{O} = \text{span}\left\{dh_j, dL_f h_j, \ldots, dL_f^{n-1}h_j\right\};\ j = 1\ldots m, \tag{7}$$

has dimension n at x_0, then the system is locally (weakly) observable. Note, $L_f^k h_j$ refers to the k-th repeated Lie derivative of the scalar function $h_j(x)$ along the vector field $f(x)$, and d is the exterior derivative. In the linear case, the observability codistribution corresponds to the observability matrix $\mathcal{O}^T = \left[C^T, A^TC^T, \ldots, (A^{n-1})^TC^T\right]$ where $C = \frac{\partial h}{\partial x}|_{x=x_0}$ and $A = \frac{\partial}{\partial x}\left(f(t,x) + g(t,x)u\right)|_{x=x_0,\ u=u_0}$.

3.2 Observability analysis of surge tank model

The aim of the observability analysis is to evaluate if measurements of either the inputs or outputs can be used to reconstruct missing measurements. Therefore, for the observability analysis, the inputs are regarded as additional states with zero dynamics.

Consider the nonlinear state space model of the surge tank in (4). Let $x_1 = v$, $x_2 = \rho$, $x_3 = q_i$, $x_4 = q_w$, $d = \rho_i$ and $\beta = q_o$. Therefore (4) becomes:

$$\begin{bmatrix} \dot{x}_1 \\ \dot{x}_2 \\ \dot{x}_3 \\ \dot{x}_4 \end{bmatrix} = \begin{bmatrix} x_3 + x_4 - \beta \\ \dfrac{x_3 d - x_2(x_3 + x_4) + x_4}{x_1} \\ 0 \\ 0 \end{bmatrix}. \tag{8}$$

The observability of the states x_1 through x_4 will be evaluated according to which of these states are measured. The observability is evaluated at the nominal operating point as shown in Table 1.

For the first measurement $y_1 = x_1$, the Lie derivatives are:

$$L_1 = \begin{bmatrix} L_f^o h_1 \\ L_f^1 h_1 \\ L_f^2 h_1 \\ L_f^3 h_1 \end{bmatrix} = \begin{bmatrix} x_1 \\ x_3 + x_4 - \beta \\ 0 \\ 0 \end{bmatrix}. \tag{9}$$

The corresponding observability matrix is:

$$\mathcal{O} = \frac{\partial L_1}{\partial x} = \begin{bmatrix} 1 & 0 & 0 & 0 \\ 0 & 0 & 1 & 1 \\ 0 & 0 & 0 & 0 \\ 0 & 0 & 0 & 0 \end{bmatrix}. \tag{10}$$

For the second measurement $y_2 = x_2$, the Lie derivatives are:

$$L_2 = \begin{bmatrix} x_2 \\ \dfrac{E}{x_1} \\ -\dfrac{E\,(2D - \beta)}{{x_1}^2} \\ (3DE - 2E\beta)\left(\dfrac{2D - \beta}{{x_1}^3}\right) \end{bmatrix}, \tag{11}$$

where $D = x_3 + x_4$ and $E = x_4 - x_2 D + d x_3$. The corresponding observability matrix as evaluated at the nominal operating point is:

$$\mathcal{O} = \frac{\partial L_2}{\partial x} = \begin{bmatrix} 0 & 1 & 0 & 0 \\ 0 & -75 & 0.01 & -0.04 \\ 0 & 5625 & -0.75 & 3 \\ 0 & -421875 & 56.25 & -225 \end{bmatrix}. \tag{12}$$

Assume the measured vector is $y = [x_1, x_2]^T$. The corresponding observability matrix can be represented as:

$$\mathcal{O} = \begin{bmatrix} 1 & 0 & 0 & 0 \\ 0 & 1 & 0 & 0 \\ 0 & 0 & 1 & 1 \\ 0 & -75 & 0.01 & -0.04 \\ 0 & 0 & 0 & 0 \\ 0 & 5625 & -0.75 & 3 \\ 0 & 0 & 0 & 0 \\ 0 & -421875 & 56.25 & -225 \end{bmatrix}. \tag{13}$$

The rank of the matrix in (13) is 4. This implies that if $x_1 = v$ and $x_2 = \rho$ are measured, $x_3 = q_i$ and $x_4 = q_w$ can be estimated. However, if only x_1 or x_2 are measured, the other states cannot be observed. This is also true if measurement of either x_3 or x_4 is used to estimate the other three states.

Table 2. Observability for different measurement sets.

Experiment#	Measured states	Fault states	Rank of $\mathcal{O}$	Observable
1	x_1	x_2&x_3&x_4	2	No
2	x_2	x_1&x_3&x_4	2	No
3	x_3	x_1&x_2&x_4	1	No
4	x_4	x_1&x_2&x_3	1	No
5	x_1&x_2	x_3&x_4	4	Yes
6	x_1&x_3	x_2&x_4	3	No
7	x_1&x_4	x_2&x_3	3	No
8	x_2&x_3	x_1&x_4	3	No
9	x_2&x_4	x_1&x_3	3	No
10	x_3&x_4	x_1&x_2	2	No
11	x_1&x_2&x_3	x_4	4	Yes
12	x_1&x_2&x_4	x_3	4	Yes
13	x_1&x_3&x_4	x_2	3	No
14	x_2&x_3&x_4	x_1	3	No

The rank of observability matrices for different combinations of measurements are given in Table 2. Specifically it indicates that unless at least both x_1 and x_2 are measured, it is not possible to observe the other states. Thus, it is expected that unless both these measurements are available, the other measurements cannot be reconstructed.

4. RECONSTRUCTION USING PCA

The aim is to investigate if the reconstruction using PCA gives similar results as the observability analysis above. The process to reconstruct missing measurements using PCA is summarized below (Dunia and Qin, 1998; Qin and Weihua, 1999; Qin and Li, 2001; Valle et al., 1999).

Consider a dataset representing normal process operation exhibiting no sensor faults $X \in \mathbb{R}^{n \times m}$ where n is the number of measurements and m is the number of sensors. Assume the dataset is scaled to zero-mean and unit variance. Dataset X can be decomposed as:

$$X = \hat{X} + \tilde{X} = TP^T + \tilde{T}\tilde{P}^T, \tag{14}$$

where $\hat{X} = TP^T$ is the model matrix, $\tilde{X} = \tilde{T}\tilde{P}^T$ is the residual matrix, and $T = [t_1, \ldots, t_l] \in \mathbb{R}^{n \times l}$ and $P = [p_1, \ldots, p_l] \in \mathbb{R}^{m \times l}$ are the score and loading matrices respectively. Vectors p_i are the principal component (PC) loadings, i.e., the eigenvectors of the covariance matrix of X, which represent how variables are related to each other. Vectors t_i are the PC scores which indicate how samples are related to each other. The cumulative percent variance (CPV) can be used as a measure to determine the number of PCs (l) in (14) to represent the most variability in the data:

$$CPV = \frac{\sum_{i=1}^{l} \lambda_i}{\sum_{i=1}^{m} \lambda_i} \times 100\%, \tag{15}$$

where λ_i are the eigenvalues corresponding to the eigenvectors p_i. A new sample vector x can be decomposed as:

$$x = \hat{x} + \tilde{x} = PP^T x + (I - PP^T)x = Cx + \tilde{C}x, \tag{16}$$

where $\hat{x} = Cx$ and $\tilde{x} = \tilde{C}x$ are the projections on the PC subspace ($\mathcal{S}_p$) and residual subspace ($\mathcal{S}_r$) respectively.

Assume x^* denotes a sample vector for normal operating conditions which is unknown when a fault occurs. The sample vector x, which contains a fault, can be represented using a normalised fault direction vector ξ_i which characterises the effect of a fault on the actual measurements:

$$x = x^* + f\xi_i, \tag{17}$$

where the scalar f represents the magnitude of the fault. For example, $\xi_i^T = [1\ 0\ \ldots\ 0]$ can represent failure in the first sensor. Fault reconstruction aims to find the best estimate of x^* in (17). The reconstruction vector x_i corrects x in the direction ξ_i such that:

$$x_i = x - f_i\xi_i, \tag{18}$$

where f_i is an estimate of the fault magnitude f. The squared prediction error (SPE) of x_i expresses the displacement between x_i and $\mathcal{S}_p$:

$$SPE_i = \left\| \tilde{C}x - f_i\tilde{C}\xi_i \right\|. \tag{19}$$

If ξ_i is known as assumed in this study, x_i can be obtained by solving the minimisation problem:

$$\min_{f_i} \|SPE_i\|. \tag{20}$$

5. RECONSTRUCTION OF MEASUREMENT ERRORS IN THE SURGE TANK

5.1 Simulation of the surge tank

The surge tank in (4) is connected in closed-loop with a linear controller (Rokebrand, 2020):

$$\begin{aligned} G_c(s) &= 100\left(G_p^{-1} + \begin{bmatrix} 33/s & 0 \\ 33/s & 0 \end{bmatrix}\right) \\ &= 100\begin{bmatrix} 0.8 + 33/s & 20\,(s+75)/s \\ 0.2 + 33/s & -20\,(s+75)/s \end{bmatrix}, \end{aligned} \tag{21}$$

where integral action is added to $G_{c_{11}}$ and $G_{c_{12}}$ to suppress steady-state volume errors. The closed-loop system is simulated using the explicit Runge-Kutta integration method for a period of 2 h with a sampling rate of 10 s. Note, since it is a common condition at the industrial plant, q_0 is kept constant at its nominal value throughout the simulation. Fig. 3 shows the closed-loop response to a series of setpoint and disturbance step changes. Process and measurement noise is not included to ensure simulated model responses are clearly visible.

5.2 PCA model of the surge tank

The PCA model of the surge tank is constructed using the surge tank simulation data for the full simulation period of 2 h. The data is first normalized to zero-mean and unit-variance. Similar to model construction in (8), a sample measurement for the PCA model is constructed as $x = [v, \rho, q_i, q_w]^T$. The resulting PC loadings and associated eigenvalues based on only two principal components are:

$$P = \begin{bmatrix} -0.43 & 0.90 \\ -0.52 & -0.18 \\ -0.52 & -0.30 \\ 0.52 & 0.27 \end{bmatrix}, \quad \lambda = \begin{bmatrix} 3.44 \\ 0.44 \end{bmatrix}. \tag{22}$$

Two principal components represent a CPV of 97% of process variability as per (15). The PCA model accuracy

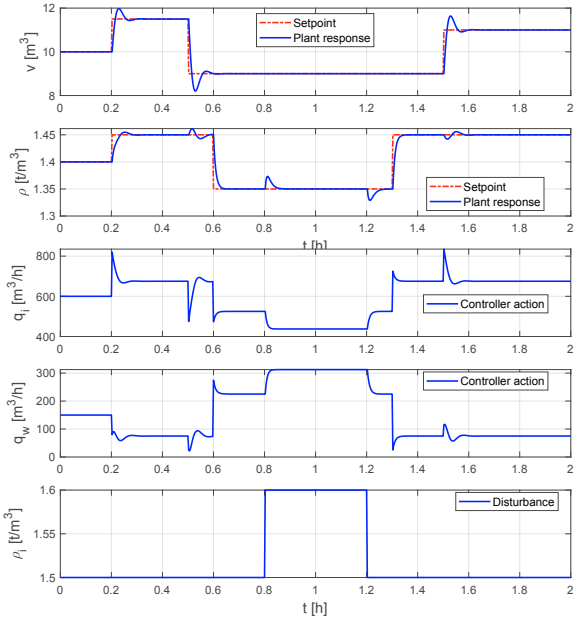

Fig. 3. Closed-loop system response.

is determined in terms of a normalized root mean square error (NRMSE):

$$NRMSE = 100\left(1 - \frac{\|x - \hat{x}\|}{\|x\|}\right), \tag{23}$$

where x is the normalized process data, and $\hat{x}$ is the PCA model. The model accuracy is shown in Table 3. This model is used for all simulations in the next section.

5.3 Reconstructing measurement faults

In this study it is assumed that the faults are identified and the direction of the faults ξ_i in (17) is known. As can be observed from the plant response directions in Fig. 3, the direction of a fault for x_4 (i.e., q_w) will be in the opposite direction as faults in the other states.

The same dataset used in Section 5.2 to construct the PCA model is used here to analyse fault reconstruction. This does not follow general practice to use two different datasets of the same process for modelling and validation (see e.g. Brooks and Bauer (2018)). However, this is done so that the PCA model can act as a benchmark to compare against the fault reconstruction accuracy.

Table 3 shows the set of experiments with the measured states, the faulty states, the fault directions, and the accuracy of reconstruction of the faulty states. Table 3 includes the observability analysis results of Table 2 for comparison. For each experiment, faults in states are simulated by replacing the relevant states with zero-value readings for the entire simulation period. At each sampling instant the minimisation problem in (20) is solved using the Nelder-Mead simplex search method and the state reconstructed according to (18). The difference between the reconstructed states and the simulated true process states is evaluated using (23).

Figs. 4-7 show the reconstruction results for Experiments 5, 7, 8 and 10 in Table 3 respectively. Similarly, Figs. 8 and 9 show results for Experiments 11 and 12 respectively.

Table 3. Model and reconstruction accuracies.

						x_1 (or v)	x_2 (or ρ)	x_3 (or q_i)	x_4 (or q_w)
					PCA model error (see (23))	2.5%	24%	19%	14%
Experi-ment#	Measured states	Faulty states	Rank of $\mathcal{O}$	Observ-able	Error direction	Reconstruction error (see (23))			
1	x_1	$x_2\&x_3\&x_4$	2	No	$\xi^T = \frac{1}{\sqrt{3}}[0,1,1,-1]$	-	86%	91%	89%
2	x_2	$x_1\&x_3\&x_4$	2	No	$\xi^T = \frac{1}{\sqrt{3}}[1,0,1,-1]$	78%	-	41%	34%
3	x_3	$x_1\&x_2\&x_4$	1	No	$\xi^T = \frac{1}{\sqrt{3}}[1,1,0,-1]$	84%	42%	-	26%
4	x_4	$x_1\&x_2\&x_3$	1	No	$\xi^T = \frac{1}{\sqrt{3}}[1,1,1,0]$	80%	34%	25%	-
5	$x_1\&x_2$	$x_3\&x_4$	4	Yes	$\xi^T = \frac{1}{\sqrt{2}}[0,0,1,-1]$	-	-	43%	36%
6	$x_1\&x_3$	$x_2\&x_4$	3	No	$\xi^T = \frac{1}{\sqrt{2}}[0,1,0,-1]$	-	40%	-	24%
7	$x_1\&x_4$	$x_2\&x_3$	3	No	$\xi^T = \frac{1}{\sqrt{2}}[0,1,1,0]$	-	33%	25%	-
8	$x_2\&x_3$	$x_1\&x_4$	3	No	$\xi^T = \frac{1}{\sqrt{2}}[1,0,0,-1]$	78%	-	-	22%
9	$x_2\&x_4$	$x_1\&x_3$	3	No	$\xi^T = \frac{1}{\sqrt{2}}[1,0,1,0]$	77%	-	30%	-
10	$x_3\&x_4$	$x_1\&x_2$	2	No	$\xi^T = \frac{1}{\sqrt{2}}[1,1,0,0]$	81%	36%	-	-
11	$x_1\&x_2\&x_3$	x_4	4	Yes	$\xi^T = [0,0,0,-1]$	-	-	-	22%
12	$x_1\&x_2\&x_4$	x_3	4	Yes	$\xi^T = [0,0,1,0]$	-	-	30%	-
13	$x_1\&x_3\&x_4$	x_2	3	No	$\xi^T = [0,1,0,0]$	-	34%	-	-
14	$x_2\&x_3\&x_4$	x_1	3	No	$\xi^T = [1,0,0,0]$	360%	-	-	-

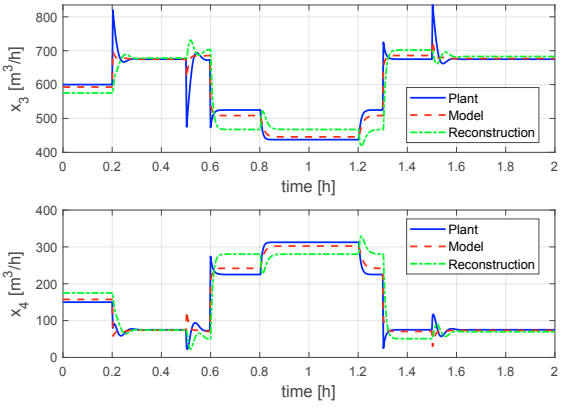

Fig. 4. Experiment 5: $x_1\&x_2$ are measured and $x_3\&x_4$ are reconstructed.

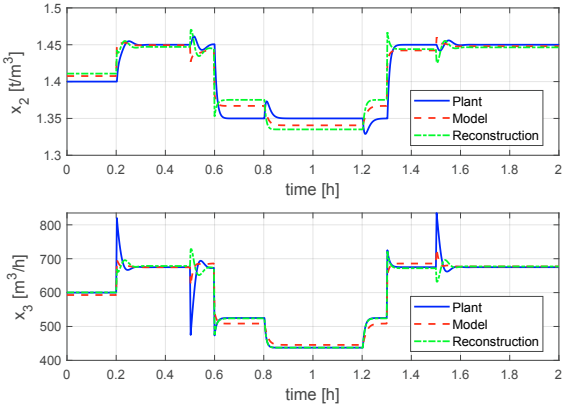

Fig. 5. Experiment 7: $x_1\&x_4$ are measured and $x_2\&x_3$ are reconstructed.

6. DISCUSSION

Table 3 indicates that for the system states to be observable, both x_1 and x_2 need to be observable. It is interesting to note that even though the system is not fully observable

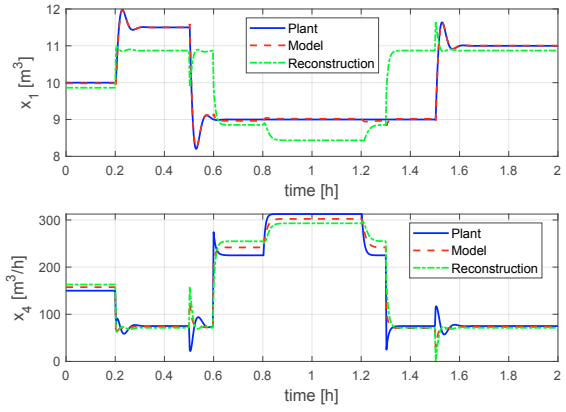

Fig. 6. Experiment 8: $x_2\&x_3$ are measured and $x_1\&x_4$ are reconstructed.

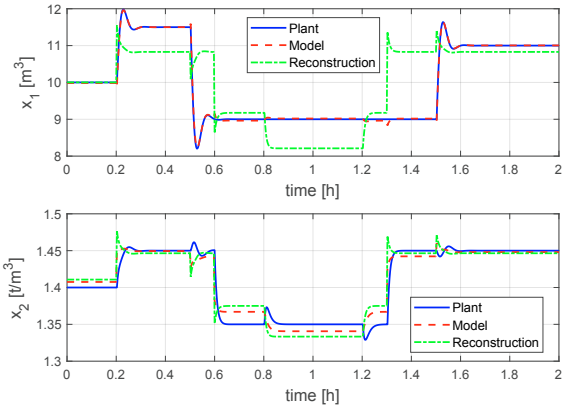

Fig. 7. Experiment 10: $x_3\&x_4$ are measured and $x_1\&x_2$ are reconstructed.

as in Experiments 6, 7, and 13, it is still possible to achieve reasonable reconstruction accuracy for x_2, x_3, and x_4 whenever at least x_1 is present. Fig. 6 for Experiment 8 and Fig 7 for Experiment 10 show the poor reconstruction of x_1.

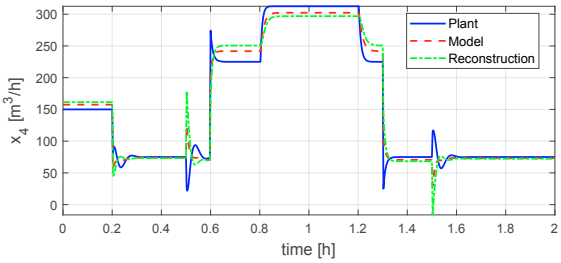

Fig. 8. Experiment 11: x_1&x_2&x_3 are measured and x_4 is reconstructed.

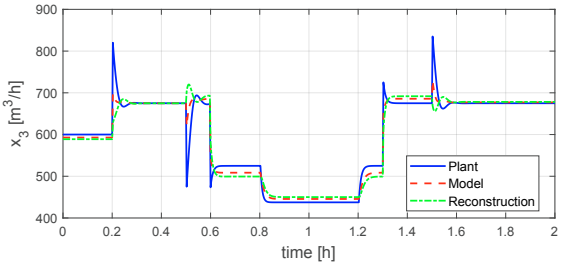

Fig. 9. Experiment 12: x_1&x_2&x_4 are measured and x_3 is reconstructed.

Table 3 indicate that whenever there is a fault in x_1, it cannot be reconstructed from the other available measurements. Although the PCA model of x_1 has the smallest error, the reconstruction error is greater than 70% for all cases where x_1 is faulty. In the PCA model in (22) the largest eigenvalue in the PCA model is more or less equally distributed among all the states, whereas the second largest eigenvalue is predominantly associated with x_1.

The largest reconstruction error for x_1 occurs for the univariate case in Experiment 14 where x_2, x_3, and x_4 are used to reconstruct x_1. However, smaller reconstruction errors occur for the multivariate cases where fewer measurements are used to reconstruct x_1. This is in contrast to the case of Brooks and Bauer (2018) where the univariate case could reconstruct faulty measurements but the multivariate cases could not be solved. Thus, rather than an error in the algorithm or approach to reconstruct faulty measurements, the dynamics of the process which determine the process models influence the ability to reconstruct faulty measurements.

7. CONCLUSION

Brooks and Bauer (2018) experienced various issues in their attempts to reconstruct measurements faults on an industrial plant using a commercially available package. The package makes use of PCA for measurement reconstruction (Dunia and Qin, 1998; Qin and Weihua, 1999; Qin and Guiver, 2003). The aim of this study is to investigate measurement reconstruction by means of PCA on a smaller scale by considering a tailings treatment surge tank. Multiple combinations of faulty and correct measurements were investigated in terms state observability and reconstruction. It appears that full observability is not necessarily required to achieve reasonably accurate reconstruction of faulty measurements. It is interesting to see that the state which is modelled most accurately by the PCA model is most difficult to reconstruct even in the univariate case where all other measurements are available. Since the problem cannot be attributed to either the algorithm or the reconstruction approach, it is concluded that it is not only the data used to construct the PCA model which influences the ability to reconstruct a measurement, but also the internal dynamics of the process as captured by the process models.

REFERENCES

Brooks, K.S. and Bauer, M. (2018). Sensor validation and reconstruction: Experiences with commercial technology. *Control Eng. Pract.*, 77, 28–40.

Burchell, J.J. and Craig, I.K. (2019). Dynamic modelling, simulation, and control of a tailings treatment surge tank. Presented at the *18th IFAC Symposium on Control, Optimization and Automation in Mining, Mineral and Metal Processing*, Stellenbosch, South Africa, 28-30 Aug. 2019.

Dunia, R. and Qin, S.J. (1998). Joint diagnosis of process and sensor faults using principal component analysis. *Control Eng. Pract.*, (6), 457–469.

Hermann, R. and Krener, A.J. (1977). Nonlinear controllability and observability. *IEEE T. Automat. Contr.*, AC-22(5), 728–740.

Hodouin, D. (2011). Methods for automatic control, observation and optimization in mineral processing plants. *J. Process Contr.*, 21(2), 211–225.

Kerschen, G., Boe, P.D., Golinval, J.C., and Worden, K. (2005). Sensor validation using principal component analysis. *Smart Mater. Struct.*, 14, 36–42.

Kullaa, J. (2010). Sensor validation using minimum mean square error estimation. *Mech. Syst. Signal Pr.*, 24, 1444–1457.

Qin, S.J. (2012). Survey on data-driven industrial process monitoring and diagnosis. *Annu. Rev. Control*, (36), 220–234.

Qin, S.J. and Guiver, J.P. (2003). U.S. patent no. 6,594,620. Washington, DC: U.S. Patent and Trademark Office.

Qin, S.J. and Li, W. (2001). Detection and identification of faulty sensors in dynamic processes. *AIChE J.*, 47(7), 1581–1593.

Qin, S.J. and Weihua, L. (1999). Detection, identication,and reconstruction of faulty sensors with maximized sensitivity. *AIChE J.*, 45, 1963–1976.

Rokebrand, L.L. (2020). *Towards an access economy model for industrial process control.* Master's thesis, University of Pretoria.

Valle, S., Li, W., and Qin, S.J. (1999). Selection of the number of principal components: The variance of the reconstruction error criterion with a comparison to other methods. *Ind. Eng. Chem. Res.*, (38), 4389–4401.

Yi, T.H., Huang, H.B., and Li, H.N. (2017). Development of sensor validation methodologies for structural health monitoring: A comprehensive review. *Measurement*, 14, 36–42.